ELSEVIER

Engineering Structures 22 (2000) 1086–1096

ENGINEERING STRUCTURES

www.elsevier.com/locate/engstruct

Hysteretic behavior of existing and retrofitted concrete-encased riveted stiffened seat angle connections

Michel Bruneau [a,*], Marc Bisson [b]

[a] *State University of New York at Buffalo, Department of Civil, Structural Environmental Engineering, Box 604300, 130 Ketter Hall, Room 212, Buffalo, NY 14260, USA*

[b] *Harmer Podolak Engineering, Nepean, Ontario, Canada*

Received 15 March 1999; received in revised form 21 July 1999; accepted 29 July 1999

Abstract

Typical riveted stiffened seat angle connections taken from a 1910 building were tested to investigate their actual hysteretic behavior and potential moment resistance and to determine how they could be efficiently retrofitted with a minimum amount of structural modifications. In that building, columns had been embedded in low-strength concrete, as typically done at the turn of the century as a fireproofing measure, and connections were tested with that fireproofing concrete left in-place. This study shows that, in their as-is condition, these existing connections can develop a considerable moment resistance, but their pinched hysteretic curves indicate that they have a relatively low energy dissipation capability. Embedment of connections in the concrete is found to be of little benefit. A steel-band/fuse-plate retrofitting scheme is proposed to improve the connection's hysteretic behavior. This retrofit technique permits the connection strength and ductility to be enhanced, without requiring removal of the column concrete cover. The effectiveness of this retrofit technique is experimentally demonstrated.

Keywords: Hysteretic behavior; Riveted stiffened seat angle connections; Retrofitting; Resistance

1. Introduction

For most of the early half of this century, resistance to wind or earthquake was not explicitly required by building codes. As a result, many buildings were constructed using steel frames having what are considered today as semi-rigid or flexible types of connections. Because concrete was often poured around the columns of those buildings for fireproofing purposes, many of these connections are also encased in concrete. Older buildings that incorporate these connections make up a large part of our infrastructure, and their seismic adequacy must be investigated.

To date, when confronted with structural evaluations of buildings having frames with semi-rigid or flexible connections, practicing engineers have conservatively neglected their potential contribution to lateral load resistance. As a result, major and sometimes intrusive seismic retrofitting have been required in such buildings. This can be costly and frequently disrupts the normal use and occupancy of the building. If it could be shown that these connections can develop some inherent moment resisting capability, in a ductile manner, their contribution to lateral load resistance could add up to be significant given that they are present in every beam-to-column connection in these old buildings. This could significantly lessen the extent of the retrofitting required, particularly in less active seismic zones. Furthermore, there is a need for localized seismic retrofit strategies that could be implemented with minimum disturbance to the occupants, and without the need to remove the column concrete encasement to expose the connections.

Although many studies (summarized in another paper [1]) have experimentally and analytically investigated the seismic adequacy of some types of semi-rigid connections, there exists little literature on the cyclic behavior and seismic retrofit of riveted stiffened seat angle connections. Two studies are particularly relevant to this paper.

* Corresponding author. Tel.: +1-716-645-2114; fax: +1-716-645-3733.

E-mail address: bruneau@acsu.buffalo.edu (M. Bruneau).

0141-0296/00/$ - see front matter
PII: S0141-0296(99)00078-4

Sarraf and Bruneau [1] cyclically tested riveted stiffened seat angle connection specimens salvaged from a 1910 building that was demolished. For this experimental investigation, the original concrete encasement was removed from the specimens. The resulting hysteretic behavior showed severe pinching in the moment rotation (M-θ) curve, indicating poor energy dissipation. The experiment ended with the shear failure of one of the rivets connecting the angle leg to the beam flange. Analytical models were developed to estimate the strength of both the top angle and the stiffened seat angle assemblies. Two other specimens were retrofitted using strategies designed to enhance energy dissipation during cyclic loading. The retrofits were successful, but required the removal of the concrete encasement.

Roeder et al. [2,3] tested a total of twenty-three specimens under monotonic and cyclic loading. All specimens were constructed from new materials to simulate the existing elements of a building located in San Francisco. The experiments included T-stub with and without web angles, as well as clip angles (or top and seat angle) with web angles. Some of the riveted connection assemblies were constructed using a specially developed in-laboratory riveting capability, while in other specimens, rivets were simulated by using mild steel bolts fitted tightly in their holes and over-tightened. Thirteen specimens had their columns and beams encased in concrete reinforced by a light welded wire mesh fabric. The original concrete used for encasement in the prototype building was designed to have a 17 MPa 28-day compressive resistance. The authors assumed that the concrete strength in the columns of that building would have increased well beyond this value over time and therefore designed the encasement concrete for their specimens to have a 24 MPa 28-day compressive strength. The results obtained from this investigation generally showed pinched M-θ curves. Many specimens with top and seat angle connections experienced shear failure of the rivets connecting the angle leg to the beam flange. The concrete encasement was reported to increase the joint strength by as much as 100% and 30% for the clip angle connections and T-stub connections, respectively, largely due to the beams developing composite action. Joint stiffness was increased by similar proportions. A rehabilitation technique for an encased connection was also tested. Angles were placed in each corner of the joint and clamped together with threaded rods. Although the resulting strength of the connection increased by approximately 25%, the M-θ curve still exhibited severe pinching. However, the "fireproofing" concrete encasing the steel columns of old buildings in eastern North America is typically considerably weaker than that tested by Roeder et al., and is usually not reinforced by welded wire mesh or otherwise. Furthermore, in those buildings, beams are frequently not encased in concrete.

This paper presents the results of cyclic testing of riveted stiffened seat angle connections encased in concrete and taken from the same existing building as considered by Sarraf and Bruneau [1]. A first test was performed on a specimen to determine the behavior of the original connection encased in concrete, while a second test was conducted on a specimen retrofitted by using a proposed steel-band/fuse-plate concept. Results are compared with capacities predicted using physical models. Although a greater number of specimens would have permitted more tests, these were the last two specimens obtained from that building.

2. Experimental approach

2.1. Materials

For this experimental study, the specimens used were salvaged from a building, built in 1910 and demolished in 1992. The structure was a seven story office building with 5 bays in the east-west direction and 8 bays in the north-south direction, each bay with an approximate span of 20 feet. The specimens obtained were flame cut from the existing frames at beam and column locations, as far as possible from the connecting elements, in order to preserve the connections.

Both specimens tested were of the top and stiffened seat angle connection type and were identical in the size and arrangement of connecting elements, column configuration as well as the amount of concrete encasement provided strictly for fire protection purposes. The typical beam-to-column connection details are shown in Fig. 1.

Coupon tests confirmed the weldability of the steel and showed an average yield strength, F_y, of 225 MPa, and an average tensile strength, F_u, of 400 MPa. Tests on rivets indicated a yield point of 258 MPa, and a tensile strength of 483 MPa. To evaluate the strength of the existing concrete, sections were removed from different areas of one of the existing specimens and three 100 mm cubes were cut from these sections with a diamond tipped saw. The three cubes averaged a compressive resistance of 8.3 MPa, which corresponds to a strength of 6.6 MPa when converted to the strength for a standard 150 mm $\times$ 305 mm cylinder based on commonly accepted relationships between values for these two different standard specimen sizes [4]. Such a low strength was expected since the quality of concrete encasing the specimens was observed to be very poor (i.e. some concrete was easily removed and most of the aggregates were porous and lightweight). It is noteworthy that the strength of the concrete used for fire proofing purposes for the columns of the building considered, when tested 86 years after being poured, was much lower than considered by Roeder et al. [2,3]. The concrete encasement in the case at hand was also totally unreinforced (i.e. no welded wire mesh or bars).

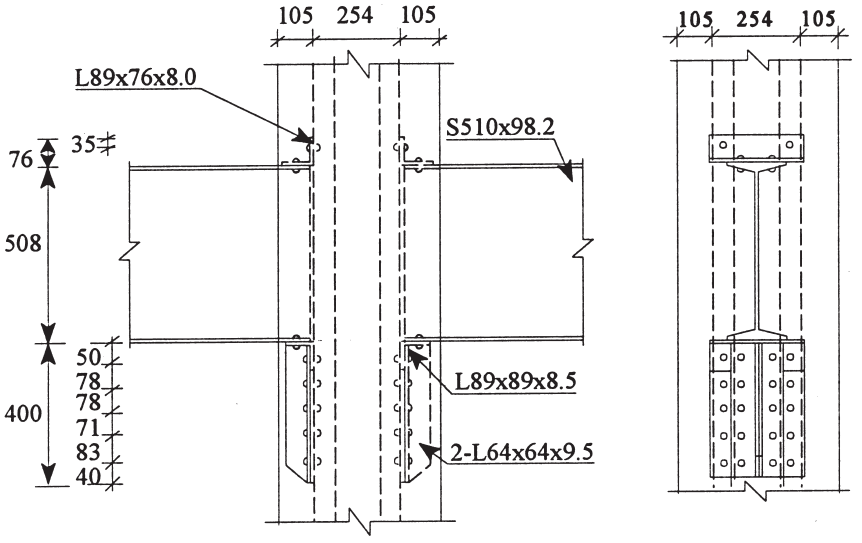

Fig. 1. Riveted stiffened seat angle beam-to-column connection detail.

The ability to duplicate this concrete strength was important because large sections of the existing concrete cover were removed in order to install strain gages to monitor the behavior of connections during testing. The concrete removed had to be replaced with a material having similar strength characteristics. Concrete mix designs of 7 MPa using normal Portland cement are no longer used in current construction practices. An alternative solution was found by using ground granulated blast-furnace slag as a replacement for normal Portland cement [5]. The replacement concrete used in the specimens was designed to have a 0.78 water/slag ratio, and a 1133/756 coarse/fine aggregate ratio with 19 mm maximum aggregate size. Cylinder compressive strengths obtained at 14 and 42 days were 6.66 and 11.8 MPa respectively, i.e. slightly higher than the results obtained from the samples extracted from the existing column encasements.

2.2. Test setup

The test set-up consists of two hinge supports, a servo-controlled actuator, and the horizontally positioned specimen. The column specimen was supported on round HSS sections rolling sandwiched between oiled steel plates, to permit unrestrained movement while being supported by the laboratory strong floor. A slotted hole was used at the end pin supports to avoid the development of axial forces in the beam from longitudinal displacement due to rigid body rotation about one of the connecting elements at the column face. Moment on each connection resulted from the product of the reaction force at the support times the lever-arm to the column face. The length of cantilever was chosen in order to produce realistic shear force on the connections, to minimize the loading capacity required of the testing equipment, and to avoid lateral torsional buckling of the beams.

The length of beams that remained in the specimens after their removal from the existing building frame were too short to fulfill these requirements. Hence, extension arms were fashioned from identical structural shapes removed from the same building. Fig. 2 shows the column with its attached stub beams and the additional extensions. Parts of these extension arms were designed to be reused for testing other specimens; slip-critical bolted splices were used for that purpose (to reduce the number of bolts required, the splices were designed to behave in double shear). Another splice in the extension arm, nearer to the column face, was welded using single bevel complete penetration welds. Further details regarding the test setup are presented elsewhere [6].

Note that the chosen test set-up is not intended to simulate the effects of earthquakes on the columns or this assembly, as the applied loading creates no shear or bending in the columns. However, the test setup definitely allows the simultaneous cyclic testing of two identical connections per specimen, and investigation of their hysteretic behavior in cases where yielding of the columns would not be an issue. The results in this paper must be interpreted in that context.

2.3. Specimen 1

This specimen was used to study the cylic behaviour of the existing connection in its as-is condition. No modifications were made to this specimen, other than the removal of some of the existing concrete in order to install strain gages on the connecting elements and replacement of the removed material using the equivalent mix described earlier.

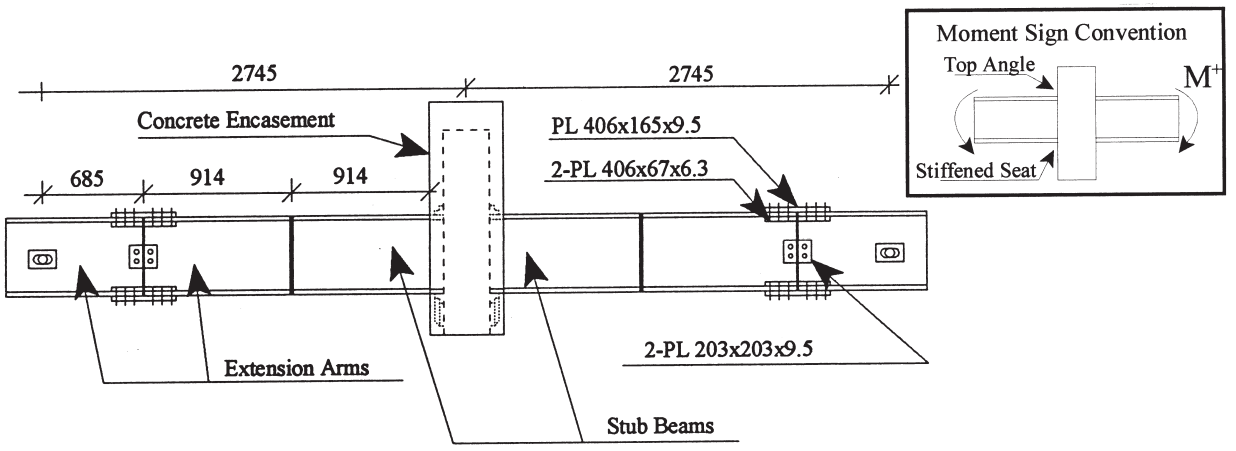

Fig. 2. Specimen test set-up.

2.4. Specimen 2

The retrofit strategy proposed in this paper follows the philosophy of localized interventions [1]. Furthermore, it minimizes disturbances by not requiring removal of the existing concrete encasement around the columns at the beam connections. It consists of steel bands wrapped around the column concrete to transfer loads to the column and "fuse-plates" acting as energy dissipators connecting the beam flanges to the steel bands, as shown in Fig. 3.

To maximize the energy dissipation provided by the new connecting elements, while respecting constraints arising from the fact that this retrofit would have to be performed on existing buildings, the following design criteria were adopted:

1. The steel-band/fuse-plate assembly must be sized to avoid contact with other structural elements in the vicinity (i.e. joists supported by beams, floor elements immediately above the beam, etc.).
2. The connection must be able to exhibit plastic rotation of at least 2% at strains not exceeding $20\epsilon_y$ in the energy dissipators.
3. Fuse-plates must be designed with a compression-to-tension strength ratio (C_r/T_r) as close as possible to 1.0 (i.e., with a low slenderness ratio, KL/r) to permit effective energy dissipation in both tension and compression when resisting the applied moments.
4. The strength of the fuse-plates must be chosen such as to preclude undesired failure mechanisms elsewhere in the structural system (i.e. plastic hinges may form in the columns if the fuses are too strong), as

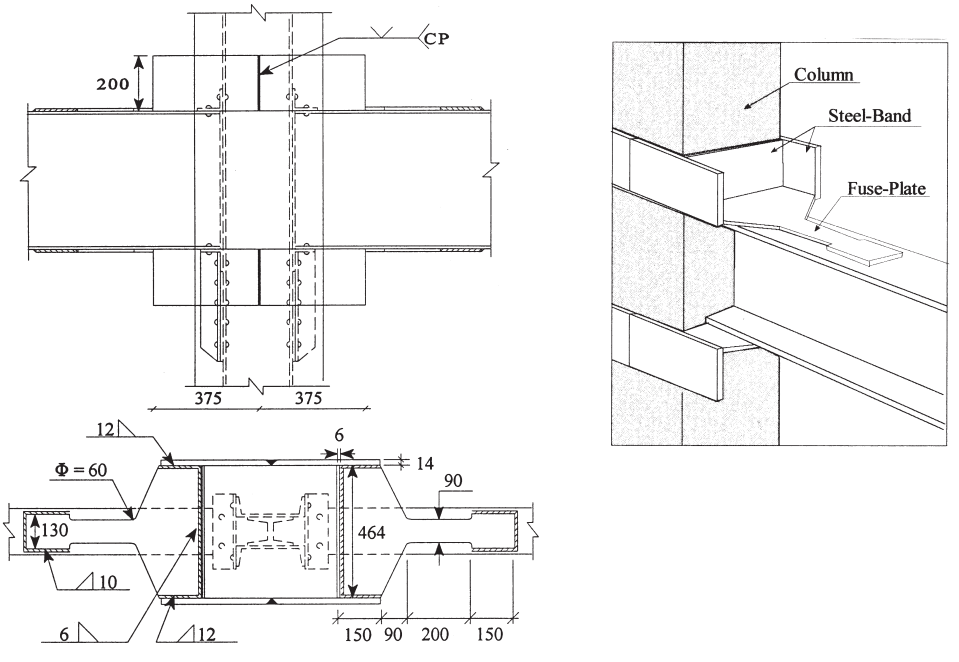

Fig. 3. Steel-band and fuse plate retrofit strategy.

well as to avoid excessive ductility demands at the expected drifts (if the fuses are too weak and unable to provide sizeable energy dissipation).

Taking the above mentioned criteria into consideration, the fuse-plates were designed to yield at a moment of 200 KN•m. This value is comparable in magnitude to the resistance of other proposed retrofit techniques for similar connection configurations [1], yet is not overwhelming compared to the capacity of the beams or column. Rounded cross-section transitions were provided at both ends of the fuses to avoid large stress concentrations in these areas. The steel-bands were designed to remain elastic.

For ease of installation, and to minimize the amount of field welding required, the steel-band/fuse-plate assembly was conceived such that two halves of the assembly could be first welded in-shop, transported to the site, and joined together with complete penetration welds. The ends of the fuse-plates connected to the beams were welded using SMAW with E70 electrodes. Welding was chosen to minimize the length of plate required, but a bolted connection is also possible (in such case, the bolts should be designed as slip critical and care must be taken to avoid net area tensile yielding in the vicinity of the bolts).

Once the steel-band/fuse-plate assembly was in place and connected to the beams, a quick setting grout with a 28-day compressive resistance of 30 MPa was poured behind the steel-band to ensure uniform contact with the column face (a non-shrink type grout is recommended, but was not used nor necessary here).

2.5. Instrumentation

Connection rotations were measured independently on each side of the column to determine the moment-rotation relationship for each connection. For verification purposes (and redundancy in the instrumentation), rotations were determined by three methods. First, by using pairs of LVDTs bolted to angles clamped to the beams measuring the distance to columns, second by using Temposonics magnetostrictive transducers to record beam deflections at fixed reference points away from the column face, and third by using readings from the displacement transducer embedded in the actuator rigidly connected to the strong floor of the laboratory. For specimen 1, the points of contact for the LVDTs on the column were square pieces of plexiglass bolted to angles which were epoxied to the column at points where concrete deterioration was not anticipated. For specimen 2, the points of contact were epoxied directly to the column faces. Connection rotations determined by the second and third methods were obtained by deducting the calculated elastic displacement of the specimen from the measured displacement and converting the resulting displacement into a rotation.

In the first experiment, the LVDTs installed at the column faces eventually went out of range and had to be removed before the specimen reached failure in order to avoid damaging the instruments. To present the entire range of test results, data from the actuator displacement was used. Correlation between the rotations calculated from the LVDTs with those calculated using the actuator displacement was good, although the latter were slightly larger due to deformations of the pin-supports and some slip in the reaction buttress.

During testing of the second specimen, problems developed in one of the two data acquisition systems and only sporadic values were recorded from the LVDTs. The few recorded rotation data obtained from the LVDTs were compared with the values calculated using the Temposonic; a good correlation was once again observed after correction to deduct setup slippage. Data recorded by the Temposonics is thus chosen to present the results of the second test.

Numerous strain gages were also installed on each specimen (including on the fuse-plates) to monitor the behavior of connections and beams. Details are presented in the research report [6].

3. Experimental results

3.1. Specimen 1

The final M-θ relationship result based on the average of nearly similar results for connections on both sides of the column is shown in Fig. 4. This specimen was subjected to twenty eight (28) cycles of loading. The hysteretic loops are visibly severely pinched, even in the early stages of the experiment. The maximum positive moment reached (M^{+}_{max}) was 59 kN•m corresponding to a maximum positive rotation (θ^{+}_{max}) of 26.7×10^{-3} radian, while the maximum negative moment (M^{-}_{max}) was

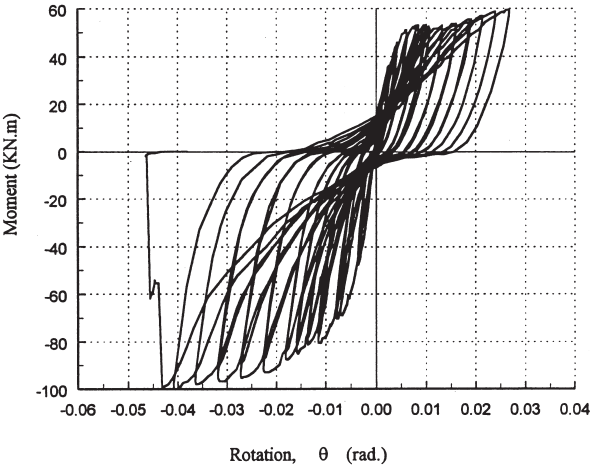

Fig. 4. Hysteretic M-θ relationship results for Specimen 1.

-100 kN•m and the maximum negative rotation (θ^-_{max}) was -43.1×10^{-3} radian. The experiment ended with the shear failure of the two rivets connecting the east beam to the stiffened seat angle.

The loading of the specimen was controlled as suggested by ATC-24 [7]. The applied force was chosen as the initial control parameter. Three cycles were first completed at $\frac{1}{2}F_y$, where F_y was based on an estimate of the connection resistance. This corresponded to $M^+=24$ kN•m with $\theta^+=1.3\times10^{-3}$ radian in positive flexure, and $M^-=-36$ kN•m with $\theta^-=-3.6\times10^{-3}$ radian in negative flexure. Small hairline cracks were visible on the concrete surface at the north-east beam-column connection location during the second cycle in positive flexure. Slight pinching was observed in these initial M-θ loops.

For the next three cycles, loading was applied up to $\frac{3}{4}F_y$, i.e. until $M^+=36$ kN•m with a corresponding $\theta^+=2.8\times10^{-3}$ radian, and $M^-=-70$ kN•m with $\theta^-=-8.1\times10^{-3}$ radian. Small cracks were observed running in the north-south direction at the level of the beam-column connection on both sides of the specimen, indicating the onset of the separation of the concrete from the steel elements. Fig. 5 shows these cracks highlighted with a black felt tip marker. Pinching and non-linearity, especially during negative flexure, were observed in the M-θ curve. After the third cycle, the regulating parameter for the flow of the experiment was changed to displacement-control.

In the next three cycles, the moment reached $M^+=45$ kN•m with a corresponding $\theta^+=4.2\times10^{-3}$ radian, and $M^-=-76$ kN•m with $\theta^-=-11.2\times10^{-3}$ radian. The same cracks observed in the previous set of cycles grew larger (approximately 2 mm in negative flexure and less than 1 mm in positive flexure). From this observation, and non-linearity observed in the negative region of the M-θ plot, the negative θ_y seemed to have been exceeded and was approximated at -4.5×10^{-3} radian.

Before proceeding with the next set of cycles, the M-θ curve showed some softening on the negative side, while the positive region was still quite linear. Therefore, the positive displacement was increased until the same softening observed in the negative region of the M-θ curve was observed in the positive portion, i.e. until $M^+=48$ kN•m and $\theta^+=6.1\times10^{-3}$ radian, while θ^- remained the same at -11.2×10^{-3} radian. In the process, the M^- corresponding to that θ^- dropped slightly to -70 kN•m, further indicating that $-\theta_y$ had been exceeded. The positive θ_y was approximated at 2.5×10^{-3} radian. At this amount of displacement, the cracks at the north and south connections were now each approximately 2 mm wide.

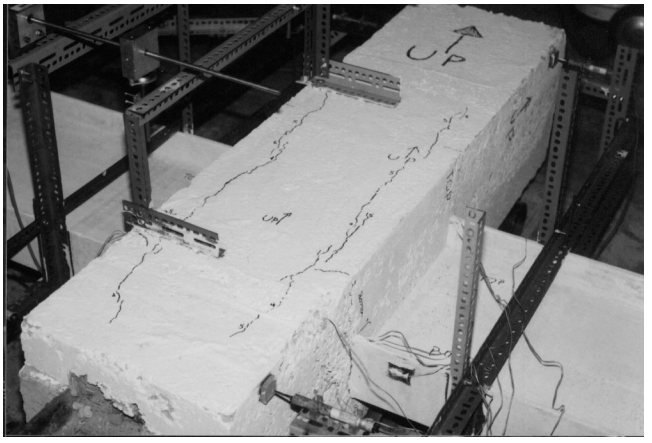

Fig. 5. Crack pattern at the onset of concrete-encasement damage for Specimen 1.

During the next three cycles, the displacements were considered to be in the range of $\pm3.0\ \theta_y$. The positive moment reached $M^+=50$ kN•m at a positive rotation $\theta^+=8.3\times10^{-3}$ radian, while the negative moment reached $M^-=-78$ kN•m at $\theta^-=-13.5\times10^{-3}$ radian. At this load level, small cracks were noticed underneath the west beam on the stiffened seat angle side. The larger cracks observed in the previous cycles continued to widen and no longer closed when the loads reversed. Pinching in the M-θ curve continued, and even seemed to get more severe.

For the next two cycles, the displacements were increased to $\pm3.5\ \theta_y$, and then to $\pm4.0\ \theta_y$ for two additional cycles. Throughout these four cycles, the cracks kept getting wider and the pinching of the M-θ curve kept getting more severe. The displacements were gradually increased in steps of θ_y, and sets of two cycles were completed for each step.

During the two cycles at a displacement of approximately $\pm7.0\Delta_y$, the positive moment reached $M^+=53$ kN•m and a positive rotation $\theta^+=18.9\times10^{-3}$ radian, while the negative moment reached $M^-=-95$ kN•m and the negative rotation $\theta^-=-31.8\times10^{-3}$ radian. The crack width was now very large, approximately 25 mm at the north end of the specimen (i.e. under positive flexure), and the LVDTs were removed to prevent their damage.

In the following cycle, severe concrete damage was observed with large crack openings and large concrete sections on the verge of falling-off. Fig. 6 shows the deterioration of the specimen at this point. In the next cycle ($\pm9.0\Delta_y$), positive moment reached $M^+=59$ kN•m at a positive rotation $\theta^+=23.9\times10^{-3}$ radian, while the negative moment reached $M^-=-100$ kN•m at a negative rotation $\theta^-=-40.8\times10^{-3}$ radian. Crack width varied between 18 to 30 mm, the higher value occurring in the vicinity of the connecting elements. In the next cycle ($\pm10.0\Delta_y$), the maximum positive moment and rotation were 59 kN•m and 26.7×10^{-3} radian, respectively, but failure occurred in negative flexure when the maximum negative moment, M^-_{max}, reached -100 kN•m and the maximum negative rotation, θ^-_{max}, -43.1×10^{-3} radian.

The concrete cover was removed after the test to visually inspect the damage. The top angles showed signs of

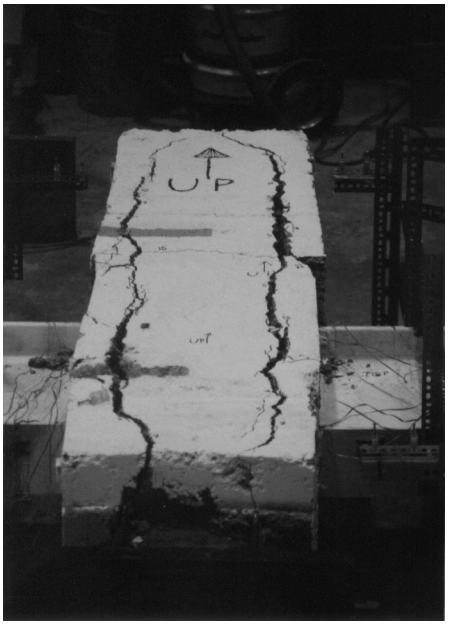

Fig. 6. Concrete-encasement damage at end of test of Specimen 1.

large inelastic excursions. The back of both angles were separated from the column face and evidence of the formation of the hinge mechanism in the vertical leg of both of the top angles was also present. The rivets of the vertical leg of the top angles showed signs of yielding and large elongations. The residual deformation of the seat angle and the stiffeners of the west side indicated that large inelastic excursions developed during the experiment.

3.2. Specimen 2

The M-θ relationship result based on the average of nearly similar results for connections on both sides of the column is shown in Fig. 7. Slight pinching is observed in the hysteretic loops at large rotations. A total of forty eight (48) cycles of loading were applied to the connection during this experiment (although 18 were in the elastic range for reasons described below). The connection developed a maximum positive moment (M^{+}_{max}) of 250 kN•m and a maximum positive rotation (θ^{+}_{max}) of 27.9×10^{-3} radian, while the maximum negative moment resisted (M^{-}_{max}) was -243 kN•m and the maximum negative rotation (θ^{-}_{max}) was -58.0×10^{-3} radian. The specimen reached failure when the north-east fuse-plate ruptured from excessive cyclic alternating plasticity due to repeated plastic buckling and tensile yielding. Fig. 8 describes the amount of buckling, or uplift from the beam flange, of the fuse-plates at different cycles.

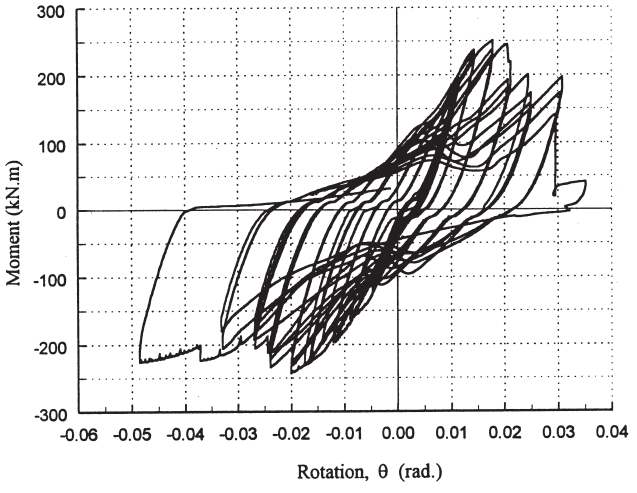

Fig. 7. Hysteretic M-θ relationship results for Specimen 2.

The specimen was initially subjected to smaller loads in the positive moment direction (due to the weaker top angle), as done in the first experiment. ATC-24 was again followed as much as possible. Sets of three cycles were completed at $\frac{1}{2}F_y$, $\frac{3}{4}F_y$, F_y, and $1.75F_y$, where F_y was that for the bare steel specimen estimated previously. At a force level of approximately 1.75 F_y, the positive moment was 77 kN•m and the positive rotation was 1.3×10^{-3} radian, while the negative moment was -128 kN•m and the negative rotation was -2.8×10^{-3} radian. At this point the M-θ curve was still linear and the specimen showed no signs of yielding.

Symmetry was also observed in the behaviour of the M-θ curve for the positive and negative resisting elements and the positive applied load was increased to equal the negative load. During the next three cycles, this action proved to be appropriate because the symmetry remained between the positive and negative cycles. The anticipated value of F_y now considered as a control parameter was changed to the F_y of the steel-band/fuse-plate assembly. The loads were gradually increased over the next two sets of three cycles each, where specimen behaviour remained elastic.

During the 19th, 20th, and 21st cycles, the value of F_y for the steel-band/fuse-plate assembly was reached, corresponding to an applied moment of M =205 kN•m and a corresponding rotation of θ =7.5×10^{-3} radian. Evidence of yielding appeared as small cracks in the paint of the narrow part of the fuse-plates, confirmed by reading in strain gages located on the fuses. Non-linearity was observed in the M-θ curve and this approximately defined the yield point (θ_y).

In the first half of the next cycle, the positive applied moment was increased to 216 kN•m and attained a rotation of 8.5×10^{-3} radian. Both fuse-plates on the south side showed slight buckling at this load level. At this point, one of the floor bolts reaction device in the test set-up failed. After a delay for design, construction, and installation of the new floor bolt supports, the experiment resumed. Since the fuse-plates had just reached yielding and only one set of the plates had buckled when the floor bolt support failed, the antici-

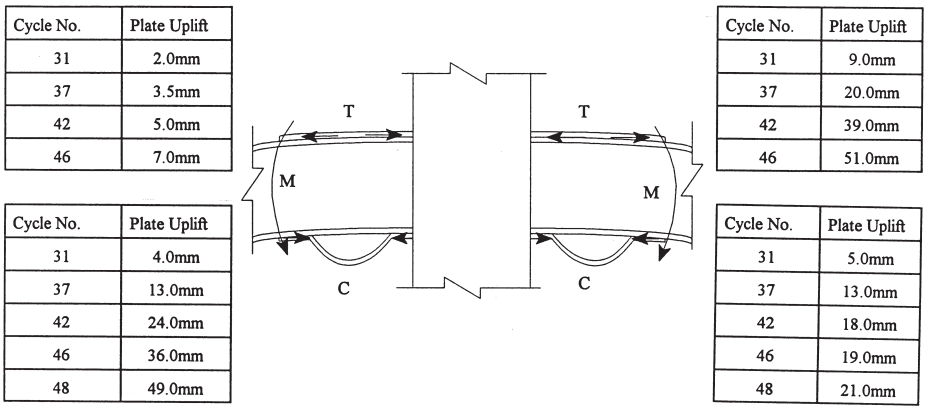

Fig. 8. Summary of fuse-plate uplift from beam flange during buckling (Specimen 2).

pated behavior of the specimen during the re-test was still expected to be a good representation of the actual retrofit behavior. Some residual deformation remained in the specimen after the previous test and the first few hysteretic loops obtained during re-test were not centred about the original axes of the M-θ graph, but after the first two sets of three cycles in the elastic range, the hysteretic loops obtained under negative and positive applied loads of identical absolute magnitude seemed to shift their centre into a more concentric location about the axes, particularly as the other fuse-plates buckled and reached the same deformation as those plates which yielded in the previous test. The cycle count in the following descriptions begins at cycle 23, since the specimen was subjected to 22 complete cycles of loading prior to resuming this test.

During cycles 29 to 31, some non-linearity was observed in the M-θ loops, especially in the negative region, at an average moment of M =165 kN•m and an average joint rotation of θ =7.5×10^{-3} radian, which is the yield displacement observed during the first part of the experiment. The fuse-plate in the north-east joint corner showed signs of slight buckling, the one in the north-west corner remained un-buckled, while both fuse-plates on the south side of the connection showed an equal amount of buckling when under compression.

After the next set of three cycles, the hysteretic loops seemed to have centred themselves about the original starting point, and the control of the experiment was changed to displacement control. The displacement was increased to what was considered to be approximately ±1.5 θ_y for cycles 35 to 37, which produced a moment M =230 kN•m and a rotation of θ =11.1×10^{-3} radian. During the first cycle at this load level, small vertical hairline cracks (in the north-south direction) formed in the concrete surface at the level of the existing connections (Fig. 9). The fuse-plates continued to yield when subjected to tension, buckle when subjected to compression, and then buckled further with each cycle. The north−east fuse-plate buckled considerably during these three cycles, lifting up from the face of the beam by up to 20 mm during the 37th cycle (Fig. 10), while the north-west plate showed very little buckling (lifting 2 to 3.5 mm). The two fuse-plates on the south side buckled by relatively the same amount, lifting at mid-length by approximately 13 mm each.

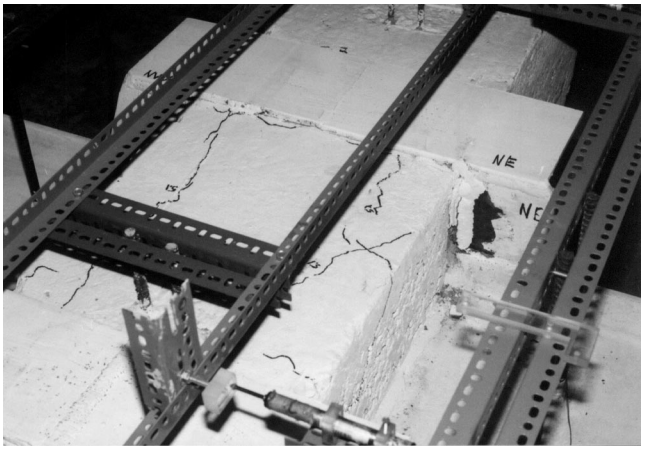

Fig. 9. Crack pattern on concrete-encasement for Specimen 2.

Fig. 10. Fuse-plate uplift from beam flange during buckling (Specimen 2).

During the 41st cycle, the displacement was increased to ±2.5 θ_y. At this level in positive bending, two sharp "snap-like" noises were heard and the applied moment dropped abruptly from 245 kN•m to 220 kN•m while the rotation increased from 17.9×10^{-3} to 19.5×10^{-3} radian. This no doubt indicated the shear failure of the two rivets connecting the top east beam flange to the outstanding leg of the top angle. These rivets were located at the north-east corner. During the following two cycles, the same displacement in the positive direction was achieved at a much lower moment (M =190 kN•m). From this point in the experiment, the stiffness and strength degradation observed in the rising segment of the M-θ curve was more pronounced. During these cycles, the east beam was sliding through the concrete encasement causing local spalling of the concrete near the north-east beam flange.

The displacement was then increased to about ±3.0 θ_y for 3 cycles, and ±3.5 θ_y for 2 cycles. Further stiffness degradation was observed in the rising segment of the M-θ curve with each cycle. Buckling deformations became large, as shown in Fig. 8. The east beam slid further through the concrete as the fuse-plate suffered additional tensile elongation, as shown by the paint marks near the large tapered end of the fuse-plate in Fig. 11. Then, the displacement was further increased to ±4.5 θ_y. During the first excursion in positive bending, the north-east fuse-plate suffered a gross area tensile failure at its mid-length where a plastic hinge had formed during buckling. The load was reversed in the hope of creating a similar failure in negative flexure, until a rotation of $\theta = -58.4\times10^{-3}$ radian was reached at a moment of $M = -226$ kN•m but no such failure occurred. More cycles of alternating plasticity would have been necessary to produce another failure; since this was not possible anymore, the experiment was terminated. The north-east and both south fuse-plates were observed to have some small evidence of necking at that point.

Fig. 11. Visible sliding of existing beam when fuse-plate is in tension, near end of test of Specimen 2.

4. Comparison and discussion of the results

4.1. Specimen 1

The M-θ relationship obtained from this experiment indicates poor energy dissipation since the hysteretic loops are severely pinched. The pinching seems to be typical of this type of connection as reported elsewhere [1–3,8]. Slippage at rivet holes, rocking of top angles, and lack of integrity of stiffened seat angles, all contribute to the pinching of the hysteretic loops and poor energy dissipation. However, this type of connection can definitely resist a non-negligible moment that might be sufficient to provide the necessary seismic resistance in small to moderate seismic zones.

The onset of top angle rivet yielding in tension is difficult to pinpoint, but experimental observations set this value at approximately 45 kN•m. At this point, significant cracking and separation of the concrete from the column was observed during testing, indicating the initial movement of the angle due to this rivet elongation. This value is close to the value calculated taking into account the effect of prying action of the top angle leg on the rivet. Development of the hinge mechanism in the top angle could not be detected by strain gages due to gage failure early during the test, but can be estimated to have initiated from a moment of approximately 50 kN•m, and have fully developed when moment reached 59 kN•m. This is relatively close to the value of 62 kN•m obtained using the top angle plastic mechanism model proposed by Sarraf and Bruneau [1].

The formation of the hinge mechanism in the stiffener angle can be observed from the experimental data to develop at approximately 80 kN•m, as confirmed by a strain gage located on the angle leg next to the column flange. This is reasonably close to the value of 76 kN•m predicted by the model of the stiffened seat connection developed by Sarraf and Bruneau [1] for bare steel. The predicted value for rivet shear failure was approximately 20% more than the experimentally obtained value (i.e., 123 compared to 100 kN•m). Since strain gage data show that these angle legs are subjected to flexure, the shear/tension interaction could have reduced the shear capacity of the rivets. Also, the diametric shrinkage, common with the cooling of field driven rivets [9], could have reduced their effective area to less than the value considered here to calculate their shear resistance.

As a general observation, the behavior and strength of this specimen does not seem to be affected by the weak unreinforced concrete encasement representative of that found in buildings built in the first half of the twentieth century in eastern north America. Although this confirms intuitively expected results, the hysteretic curves for this specimen provide a needed benchmark against which behavior of the retrofitted specimen can be compared.

4.2. Specimen 2

As revealed by comparing their experimentally obtained moment-curvature hysteretic curves, the retrofitted specimen shows an enhanced hysteretic behavior compared to the non-retrofitted one. The M-θ relationship for the retrofitted connection exhibits larger strength and hysteretic energy dissipation, although some pinching developed at large joint rotations. Even though the fuse-plates were designed to have nearly identical tensile yielding and compressive buckling strengths, stiffness degradation is unavoidable for such systems at large rotations. This is because tensile yielding increases the length of the fuse-plates; when the load is reversed, buckling occurs earlier than in the previous cycle because the elongated plates must be compressed to fit in their original position. As the loading progresses, buckling occurs earlier in each subsequent cycle than in the previous one. As the buckled plate straightens, the tensile resistance can be developed anew, but this will occur at progressively larger drifts. In hindsight, the proposed retrofit concept can be improved by adding simple devices to reduce the slenderness of the fuse-plates while keeping them free to elongate: for example, U-shaped bars bolted to the existing beam flanges, each straddling a fuse-plate at its mid-length or at more frequent intervals, would likely eliminate some of the observed pinching by forcing yielding to occur in axial compression instead of through inelastic buckling. Alternatively, when appropriate clearances are available, the fuses could be designed to rely on plates in bending, as proposed in other applications [10].

During this experiment, the yielding of the fuse-plates occurred when the applied moment was 208 kN•m. There is very good agreement between the experimental value and the expected yield value of 192 kN•m, given by the product of the tensile yield force ($T_r = A_s \times F_y$ =1260 mm^2 × 300 MPa =378 kN) and the beam depth (0.508 m). This seems to indicate that the existing connection, being significantly more flexible than the steel-band fuse-plate assembly, contributed only slightly to the overall specimen strength prior to yielding. Unfortunately, the strain gages necessary to quantify this contribution from the existing beam failed early during the test.

Again, the concrete encasement was not found to provide any significant additional resistance to the connection. However, results indicate that the confinement provided by the steel-band allows the transfer of loads to the column by maintaining the integrity of the connection, even after the existing elements of the connection have failed. The steel-band assembly also prevents the concrete encasement from cracking or spalling until large rotations have been attained.

5. Conclusions and recommendations

From this experimental study of the hysteretic behavior of existing riveted stiffened seat angle connections encased in concrete, and proposed techniques for their seismic retrofit, it can be concluded that:

- Although riveted stiffened seat angle connections have not been designed to resist moments, they can develop a considerable moment capacity and exhibit a relatively ductile hysteretic behavior which could be beneficially considered when evaluating frames built of these connections and subjected to small and moderate earthquakes. However, they exhibit pinched hysteretic curves, and retrofitting may be desirable. Similar behavior is expected for identical connections having mild bolts (of strength comparable to that of rivets) instead of rivets, with possibly more pinching in the hysteretic loops due to greater slippage within the bolts holes.
- Column concrete encasement of the type tested here, and representative of what is frequently found in eastern North-America, does not increase the strength of the riveted stiffened seat angle connections.
- The proposed steel-band/fuse-plate seismic retrofit strategy is an effective solution that enhances moment capacity and significantly improves the hysteretic energy dissipation capability of these riveted stiffened seat angle connections, without the need to remove the concrete-encasement of the column. However, awaiting the results of non-linear inelastic analysis of full structures, engineers are cautioned to use judgment and pay particular attention to drift and P-Δ issues when using these retrofit solutions.

Acknowledgements

The writers are grateful for the cooperation of Peter McCourt of National Capital Commission, John Cooke, of John Cooke and Associates Ltd., and Paul Greenspoon, of Greenspoon Bros. Ltd, for their cooperation in obtaining the test specimens from the demolished Daly building in Ottawa. This research program was partly funded by the Natural Science and Engineering Research Council of Canada. This support is sincerely appreciated. However, the opinions expressed in this paper are those of the writers and do not reflect the views of the aforementioned sponsor or individuals.

References

[1] Sarraf M, Bruneau M. Cyclic testing of existing and retrofitted riveted stiffened seat angle connections. ASCE Structural Journal 1996;122(7):762–75.

[2] Roeder CW, Leon RT, Preece FR. Strength, stiffness and ductility of older steel structures under seismic loading. Structural and Geotechnical Engineering and Mechanics Report No. SGEM 94-4. Department of Civil Engineering, University of Washington, Seattle, Washington, 1994.
[3] Roeder CW, Knechtel B, Thomas E, Vaneaton A, Leon RT, Preece FR. Seismic behavior of older steel structures. ASCE Structural Journal 1996;122(4):365–73.
[4] Neville AM. Properties of concrete. England: Longman Group Limited, 1995.
[5] Malhotra VM. Mechanical properties and freezing and thawing durability of concrete incorporating a ground granulated blast-furnace slab. CANMET report 0705-5196, 86-10E. Ottawa: CANMET, Energy, Mines and Resources, 1988.
[6] Bisson MA, Bruneau M. Experimental study on cyclic behavior of riveted stiffened seat angle connections with concrete encasement, Ottawa Carleton Earthquake Engineering Research Centre report OCEERC 98-19. Department of Civil Engineering, University of Ottawa, Ottawa, Canada, 1998.
[7] Applied Technology Council. ATC-24 guidelines for cyclic seismic testing of components of steel structures. Redwood City, California: Applied Technology Council, 1992.
[8] Bernuzzi C, Zandonini R, Zanon P. Semi-rigid steel connections under cyclic loads. Proceedings of the First World Conference on Constructional Steel Design, Acapulco, Mexico, 1992.
[9] Kulak GL, Fisher JW, Struik JHA. Guide to design criteria for bolted and riveted joints. 2nd ed. New York: John Wiley and Sons, 1987.
[10] Tsai K-C, Chen H-W, Hong C-P, Su Y-F. Design of steel triangular plate energy absorbers for seismic-resistant construction. Earthquake Spectra 1993;9:505–28.